Malaysian Journal of Chemistry, 2020, Vol. 22(3), 76-88
(Special Issue: *International Conference in Organic Synthesis - ICOS 2019, Universiti Teknologi MARA*)

Synthesis of Some Novel Pyrrolidine-Based Iminosugars, Molecular Docking Study and Evaluation of Their Antidiabetic Properties

Wibowo A.[1], Shaameri Z.[2], Mohammat M. F.[2], Rashid F. N. A. A[2], Rezali N. S.[3], Kamarulzaman F.[4] and Hamzah A. S.[2]*

[1]Faculty of Applied Science, Universiti Teknologi MARA (UiTM) Pahang, Jengka Campus, 26400 Bandar Tun Abdul Razak Jengka, Pahang, Malaysia
[2]Organic Synthesis Laboratory, Institute of Science, Universiti Teknologi MARA (UiTM), 42300 Bandar Puncak Alam, Selangor Darul Ehsan, Malaysia
[3]Chemical Sciences Programme, School of Distance Education, Univesiti Sains Malaysia (USM), 11800 Minden, Penang, Malaysia
[4]Forest Research Institute Malaysia (FRIM), Kepong, 52109 Selangor Darul Ehsan, Malaysia
*Corresponding author (e-mail: asazali@uitm.edu.my)

Eleven pyrrolidine-based iminosugar derivatives have been synthesized and evaluated for inhibition of α-glucosidase and molecular docking. The compounds studied were hydrazinyl, hydroxyamino and hydroxypyrrolidine derivatives. The most promising iminosugar derivative was 3-hydrazinyl-4-hydroxymethyl-1-methyl-5-(4-methoxyphneyl) pyrrolidine (C**oS-10**), giving an IC_{50} of 1.116 ± 1.01 mM. The hydrazine group at C-4 and methoxybenzene ring at C-2 seemed to play important roles in the activity of **CoS-10**. Docking studies showed that all the compounds occupied the same region as the DNJ inhibitor on the enzyme binding site with the most active compounds establishing similar interactions with key residues. Despite the fact that activity was found only in the mM range, this study demonstrated that the newly synthesized compounds had promising effects in inhibiting α-glucosidase, so that inhibition can be improved in further studies.

Key words: Iminosugar; pyrrolidine; α-glucosidase; molecular docking; antidiabetic

Received: December 2019; Accepted: May 2020

In living beings, both the glycosidases and glycosyltransferases are used for controlling biosynthesis of oligosaccharides and glycoconjugates [1]. Consequently, oligosaccharides and glycoconjugates play major roles in various cellular functions such as cell adhesion, cell differentiation, and other metabolic disorders and diseases. The development of these glucosidase inhibitors is of great importance, therefore, an immense growth in the design, synthesis, and biological evaluation of glycosidase inhibitors have been reported [2]. Among the reported inhibitors, polyhydroxylated nitrogen-containing heterocycles (iminosugars and azasugars) have been the target compounds in organic synthesis in recent years [3].

Some glycosidase drugs available in the market include *N*-hydroxyethyl-1-deoxynojirimycin (miglitol) and *N*-butyl-1-deoxynojirimycin (miglustat) which have been used in the treatment of Diabetes type II and Gaucher's disease, respectively [4]. Besides that, pyrrolidine-based iminosugars (azasugars) such as 1,4-dideoxy-1,4-iminohexitol (iminohexitol) and 1-butyl-1,4-dideoxy-1,4-imino-arabinitol (iminoarabinitol) as well as their analogs have been reported to be potent glycosidase inhibitors (**Fig. 1**) [5-7]. It has also been shown that the variation of the hydroxyl groups in the skeletal structures has profound effects on their biological activities.

Recently, some synthetic approaches of these biologically active pyrrolidine-based iminosugars have been reported [8, 9]. However, very few reports are known on the preparation of pyrrolidine-based iminosugars through multi-component reactions (MCR).

As part of our ongoing research project in our laboratory on pyrrolidine type of compounds [10-15], we herein report the synthesis of several new pyrrolidine-based iminosugar derivatives in search of new potential glucosidase inhibitors. All synthesized compounds were evaluated for α-glucosidase inhibitory activity; the existence of interactions between synthesized compounds (inhibitors) and α-glucosidase through molecular docking study was also investigated.

†Paper presented at the International Conference in Organic Synthesis (ICOS 2019), 9-10 December 2019, Universiti Teknologi MARA.

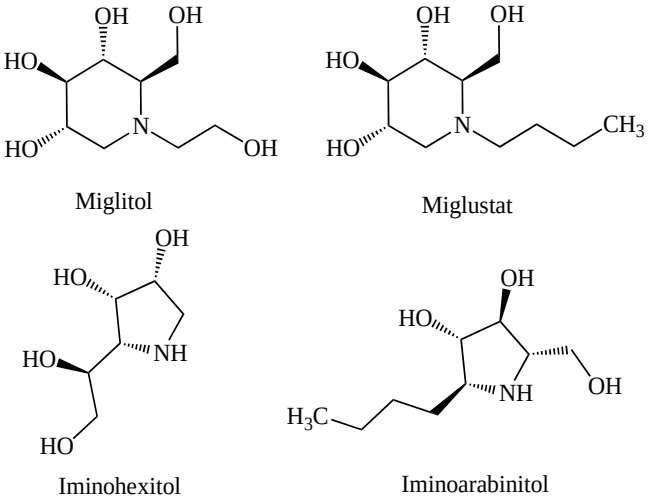

Figure 1. Structures of some biologically active iminosugars available in the market.

MATERIALS AND METHODS

1. Computational Simulations

1.1. Preparation and optimization of ligands

A series of compounds were constructed using Marvin Sketch version 1.5.6 (ChemAxon, Budapest, Hungary). These ligand structures were converted into 3D structures and geometrically optimized with OPLS3 using Ligand Preparation Wizard (Schrodinger, New York, USA).

1.2. Homology modelling

Homology model of α-glucosidase from *Saccharomyces cerevisiae* was built using Prime (Schrodinger, New York, USA). The protein sequence of *Saccharomyces cerevisiae* α-glucosidase in FASTA format was retrieved from National Center for Biotechnology Information (NCBI) (http://www.ncbi.nlm.nih.gov). Template sequences for development of homology model were identified from Protein Database Bank (PDB) (http://www.rcsb.org) using BLAST homology search and both sequences were aligned using Clustal Omega 1.2.4. [16]. The highest similarity sequence was selected for homology modelling. Then, the sequences were aligned and the model was generated by energy-based algorithm. The modelled structure was evaluated by Ramachandaran plot using RAMPAG (http://mordred. bioc.cam.ac.uk/~rapper /rampage.php).

1.3. Preparation and optimization of protein receptors

The homology structure model of *Saccharomyces cerevisiae* α-glucosidase was optimized and minimized using Protein Preparation Wizard (Schrodinger, New York, USA). Hydrogen atoms were added in its standard geometry, adjusting the bond orders and formal charges and the structure was refined by optimization and minimization of the geometries until the average root mean square deviation (RMSD) of non-hydrogen atoms reached 0.3 Å using OPLS3 force field.

1.4. Generation of receptor grid files

Receptor grids were calculated for prepared proteins such that various ligand poses bind within the predicted active site during docking. Grids were generated by keeping the default parameters of van der Waals scaling factor 1.00 and charge cut-off 0.25 subjected to OPLS 2003 force field. A cubic box of specific dimensions was generated by setting at the coordinate of X=, Y= and Z= for the receptor. The bounding box was set to 20 Å × 20 Å × 20 Å for docking experiments.

1.5. Molecular docking

Molecular docking was performed to investigate the binding modalities of ligands toward the target of glucose-α-glucosidase. Molecular docking simulations were performed using GLIDE as part of the Schrodinger Small Molecule Drug Discovery Suite 2017-1 software (New York, USA). Co-crystallized ligands were re-docked as validation of the docking protocol. Docked structures were visualized using PyMOL (http://www.pymol.org). Two-dimensional schematic representation of protein-ligand interaction was generated using Ligand Interaction Diagram version 1.97.0 (Schrodinger, New York, USA).

1.6. Pharmacological properties of the compounds

ADMET properties of all compounds were predicted using QikProp in Schrodinger Small Drug Discovery Suite-2017 (New York, USA). QikProp calculated 44 descriptors of the compounds. The difference of chemical descriptors for the pharmacokinetics properties were calculated to check the compliance of studied compounds with the recommended values.

2. Determination of α-glucosidase Inhibition Activity

α-glucosidase enzyme inhibitory activity assay was adopted from the method described by Lee *et al.*[17] with slight modifications. α-glucosidase from *Saccharomyces cerevisiae* (EC 3.2.1.20, Sigma-Aldrich, St. Louis, USA) was dissolved in cold phosphate buffer saline, pH 6.5. *p*-nitrophenyl-α-D-glucopyranoside was prepared in the same buffer and used as substrate solution. Sample (10 µL), enzyme (20 µL), water (20 µL) and buffer (40 µL) were mixed in a microtiter plate and pre-incubated at 37°C for 10 minutes. Then, absorbance was measured at 405 nm using a spectrophotometer (Epoch 2, BioTek). 10 µL of substrate solution was added immediately and the plate was further incubated at 37°C. The absorbance was measured again after 30 minutes of incubation. The final reaction mixtures contained various concentrations of sample, 0.1 U/mL enzyme, and 1.25 mM substrate. Percentage of enzyme inhibition was calculated from ratio of sample absorbance changes within 30 minutes over control absorbance. IC_{50} value was obtained from non-linear regression analysis (Sigmoidal-4PL) using GraphPad Prism 5 (GrapPad Software, California, USA).

3. Compound Synthesis

3.1. General information

High resolution mass spectra were obtained from Agilent 1290 Infinity LC system coupled to Agilent 6520 Accurate-Mass Q-TOF. The ^{1}H and ^{13}C-NMR spectra were registered in $CDCl_3$ with Joel Resonance ECZ400S [400 MHz (^{1}H) and 100 MHz (^{13}C)] using TMS as the internal standard. Analytical TLC was performed on silica gel 60 F_{254}, Merck (layer thickness 0.25 mm, Merck) and visualized with UV light and $KMnO_4$ as the detecting agent.

3.2. General procedure for the synthesis of pyrrolidine intermediates (1a-e)

A suspension of sodium diethyl oxaloacetate (1 eq), amine solution in absolute ethanol (1 eq), and aldehyde (1 eq) in ethanol was heated at reflux towards complete solution (0.5-2 h). After cooling, the mixture was added into ice-water and then acidified with HCl. The precipitate was filtered, washed with water and ether in order to remove traces of aldehyde to yield pyrrolidine (**1a-e**).

3.2.1. Synthesis of ethyl 3-hydroxyamino-4-pyrrolidine carboxylate (2a)

To the solution of pyrrolidine **1a** (1.5 g, 8.82 mmol) in 100 mL of dichloromethane was added hydroxylamine hydrochloride (0.74 g, 10.59 mmol), sodium bicarbonate (1.07 g, 12.71 mmol), and sodium sulphate (1.8 g, 12.71 mmol). The mixture was stirred at room temperature for 24 h, filtered and evaporated to furnish hydroxyamino pyrrolidine **2a** as a white solid in quantitative yields.

3.3. General procedure for the synthesis of pyrrolidine intermediates (3a-e)

Hydrazine hydrate (5.8 mmol) was added to a mixture of 2,3-dioxo-4-carboxy-5-(substituted)pyrrolidines (2.9 mmol), acetic acid (2.9 mmol), and 15 mL of ethanol. The mixture was stirred overnight at room temperature. The resulting precipitate was filtered from the reaction and washed with ethanol to give a white precipitate **2-CoS-5**. For **2-CoS-8-10**, the reaction mixtures were evaporated under reduced pressure, extracted with EtOAc, washed with H_2O, dried over $MgSO_4$, and evaporated to afford the products.

3.3.1. Synthesis of 5-(4-methoxyphneyl)-1-methyl pyrrolidine-2,3-dione (4e)

Pyrrolidine **1e** (0.20 g, 0.77 mmol) was dispersed in 10% aqueous hydrochloric acid solution (10 mL) and heated under reflux for seven hours, which gradually dissolved to give a brownish solution. The reaction mixture was then cooled and concentrated to dryness. The crude product was triturated with diethyl ether and extracted with DCM and water. The organic layer was dried over $MgSO_4$, filtered, and concentrated in vacuo to give the pure product pyrrolidinone (**4e)** (75% yield).

3.4. General procedure for the synthesis of iminosugars CoS-(1-11)

To the stirred solutions of **1a-e**, **2a**, **3a-e**, and **4e** in ethanol were added catalytic amount of Pd-C (10% wt.) (0.3 eq) and acetic acid (2 eq). The reactions were stirred vigorously under hydrogen atmosphere for 24 h and then filtered through Celite. After removal of the solvent, the pure solid products were washed with ether and recrystallized in methanol-chloroform, while the impure solid products were purified using silica gel column chromatography eluted with hexane-ethyl acetate before submitted to the next steps.

The pure products obtained were dissolved in dry tetrahydrofuran, and were added slowly to the solution of lithium aluminium hydride (excess) in 50

mL round bottom flasks. The mixtures were heated at 90ºC for 4-6 h and then cooled to 0°C. The reaction mixtures were quenched by the addition of distilled water, and the mixtures were filtered through Celite and concentrated in vacuo to give the pure products of iminosugar derivatives **CoS-(1-11)** as solids after recrystallization or purification by column chromatography.

*3-hydroxy-4-hydroxymethyl pyrrolidine (**CoS-1**)*: White solid; 90%. HRESI-MS *m/z*: $[M+H]^+$ 118.0674 (Calc. for $C_5H_{12}NO_2$, 118.0862). ^{1}H-NMR (DMSO-D_3, 400 MHz) δ 3.52-3.40 (3H, *m*, CHOH and CH_2OH), 3.41-3.25 (4H, *m*, 2 x $NHCH_2$), 1.53 (1H, *sx*, *J*= 5.6 Hz, CH). ^{13}C-NMR (DMSO-D_3, 100 MHz) δ 46.2, 59.8, 60.3, 64.8 and 70.6.

*3-hydroxy-4-hydroxymethyl-1-methyl pyrrolidine (**CoS-2**)*: Brown solid; 90%. HRESI-MS *m/z*: $[M]^+$ 131.0908 (Calc. for $C_6H_{13}NO_2$, 131.0941). ^{1}H-NMR (CD_3OD, 400 MHz) δ 3.52-3.40 (3H, *m*, CHOH and CH_2OH), 4.35 (1H, *dt*, *J*= 5.2, 4.4 Hz, CHOH), 3.77 (1H, *dd*, *J*= 8.0, 11.2 Hz, OCH_2-a), 3.60 (1H, *dd*, *J*= 6.8, 11.2 Hz, OCH_2-b), 3.01 (1H, *dd*, *J*= 5.6, 10.4 Hz, NCH_2-a CHOH), 2.79 (1H, *dd*, *J*= 8.0, 9.2 Hz, NCH_2-a), 2.44 (1H, *m*, NCH_2-b CHOH), 2.41 (1H, *m*, NCH_2-b), 2.34 (3H, *s*, NCH_3) and 1.61 (1H, *m*, CH). ^{13}C-NMR (CD_3OD, 100 MHz) δ 41.6, 45.3, 57.5, 60.3, 64.2 and 71.3.

*5-ethyl-3-hydroxy-4-hydroxymethyl-1-methylpyrroli dine (**CoS-3**)*: Brown solid; 85%. HRESI-MS *m/z*: $[M]^+$ 159.9179 (Calc. for $C_8H_{17}NO_2$, 159.1254). ^{1}H-NMR (CD_3OD, 400 MHz) δ 1.07 (3H, *t*, *J*= 7.2 Hz, CH_3), 1.86 (2H, *sx*, *J*= 7.2 Hz, CH_2), 2.54 (1H, *dt*, *J* = 7.6, 13.2 Hz, NCH), 2.80 (3H, *s*, NCH_3), 3.13 (1H, *dd*, *J* = 6.0, 12.0 Hz, NCH_2-a), 3.46 (1H, *dd*, *J* = 3.2, 11.6 Hz, NCH_2-b), 3.79 (1H, *dd*, *J*= 6.0, 10.8 Hz, OCH_2-a), 3.83 (1H, *dd*, *J*= 6.0, 10.8 Hz, OCH_2-b) and 4.53 (1H, *dd*, *J*= 5.6, 9.2 Hz, CHOH). ^{13}C-NMR (CD_3OD, 100 MHz) δ 10.4, 21.1, 41.2, 46.1, 56.2, 62.9, 69.2 and 71.4.

*3-hydroxy-4-hydroxymethyl-1-methyl-5-(4-methoxy phneyl) pyrrolidine (**CoS-4**)*: Brown solid; 78%. HRESI-MS *m/z*: $[M]^+$ 237.1249 (Calc. for $C_{13}H_{19}NO_3$, 237.1359). ^{1}H-NMR (CD_3OD, 400 MHz) δ 2.07 (3H, s, NCH_3), 2.22 (1H, *m*, CH), 2.71 (1H, *d*, *J*= 9.2 Hz, NCH_2-a), 3.13 (1H, *t*, *J*= 7.6 Hz, NCH_2-b), 3.32 (1H, *m*, NCH), 3.36 (1H, *dd*, *J*= 6.4, 10.8 Hz, OCH_2-a), 3.47 (1H, *dd*, *J*= 4.0, 10.8 Hz, OCH_2-b), 3.76 (3H, *s*, OCH_3), 3.80 (1H, *m*, CHOH), 6.87 (2H, *d*, *J*= 8.4 Hz, Ar-CH) and 7.24 (2H, *d*, *J*= 8.4 Hz, Ar-CH). ^{13}C-NMR (CD_3OD, 100 MHz) δ 39.2, 49.4, 54.3, 55.6, 62.6, 73.5, 113.6, 129.0, 132.3 and 159.5.

*3-hydroxyamino-4-hydroxymethyl pyrrolidine (**CoS-5**)*. Brown solid; 70.4%. HRESI-MS *m/z*: $[M]^+$ 132.0428 (Calc. for $C_5H_{12}N_2O_2$, 132.0893). ^{1}H-NMR (DMSO-D_3, 400 MHz) δ 3.52-3.40 (2H, *m*, CH_2OH), 3.41-3.25 (4H, *m*, 2x$NHCH_2$), 2.6 (1H, *m*, HONHCH), 1.35 (1H, *m*, CH). ^{13}C-NMR (DMSO-D_3, 100 MHz) δ 22.6, 26.0, 29.2, 31.8, 33.0 and 61.2.

*3-hydrazinyl-4-hydroxymethyl pyrrolidine (**CoS-6**)*. Pale yellow solid; 93%. HRESI-MS *m/z*: $[M]^+$ 131.0853 (Calc. for $C_5H_{13}N_3O$, 131.1053). 1H-NMR (D_2O, 400 MHz) δ 3.35-3.19 (2H, *m*, CH_2OH), 3.21-3.01 (4H, m, 2 x NCH_2), 1.28 (1H, *m*, CH). ^{13}C-NMR (D_2O, 100 MHz) δ 44.5, 58.7, 59.2, 63.4 and 70.2.

*3-hydrazinyl-4-hydroxymethyl-1-methyl pyrrolidine (**CoS-7**)*. White solid; 90%. HRESI-MS (negative mode) *m/z*: $[M-H]^-$ 144.0791 (Calc. for $C_6H_{14}N_3O$, 144.1142). ^{1}H-NMR (CD_3OD, 400 MHz) δ 3.85-3.90 (2H, *m*, CH_2OH), 3.80 (1H, m, NH_2NHCH), 3.70-3.50 (4H, m, 2 x NCH_2), 2.80 (3H, *s*, NCH_3), 1.80 (1H, *m*, CH). ^{13}C-NMR (D_2O, 100 MHz) δ. 53.4, 55.9, 59.4, 62.1, 68.8 and 71.2.

*3-hydrazinyl-4-hydroxymethyl-1,5-imethylpyrrolidine (**CoS-8**)*. White solid; 95%. HRESI-MS MS (negative mode) *m/z*: $[M+H]^+$ 159.0902 (Calc. for $C_7H_{17}N_3O$, 159.1377). ^{1}H-NMR (CD_3OD, 400 MHz) δ 0.94 (1H, *d*, *J*=7.2 Hz, CH_3), 1.70 (1H, *m*, CH), 2.27 (3H, *s*, NCH_3), 2.33 (1H, *m*, NCH), 3.41 (1H, *dd*, *J*= 4.8, 11.6 Hz NCH_2-a), 3.55 (1H, *m*, NCH_2-b), 3.58 (1H, *q*, *J*= 7.2 Hz, NH_2NHCH), 3.72 (1H, *dd*, *J*= 5.2, 10.8 Hz, OCH_2-a), 3.84 (1H, *dd*, *J*= 7.2, 10.8 OCH_2-b). ^{13}C-NMR (CD_3OD, 100 MHz) δ 9.24, 46.2, 55.9, 60.4, 63.9, 69.2 and 72.4.

*5-ethyl-3-hydrazinyl-4-hydroxymethyl-1-methyl pyro lidine (**CoS-9**)*. White solid; 90%. HRESI-MS (negative mode) *m/z*: $[M+K-2H]^-$ 210.9579 (Calc. for $C_8H_{17}N_3OK$, 210.1014). ^{1}H-NMR (DMSO-D_3, 400 MHz) δ 1.06 (1H, t, *J*=7.2 Hz, CH_3), 1.75 (2H, qt, *J*=7.2 Hz, CH_2), 2.01 (1H, *m*, CH), 2.19 (1H, *q*, *J*= 5.6, NCH), 2.90 (3H, s, NCH_3), 3.10 (1H, *m*, NCH_2-a), 3.24 (1H, *m*, NCH_2-b), 3.44 (1H, *m*, NH_2NHCH), 3.52 (1H, *dd*, *J*= 5.2, 10.8 OCH_2-a), 3.66 (1H, *dd*, *J*= 4.8, 10.8 OCH_2-b). ^{13}C-NMR (DMSO-D_3, 100 MHz) δ 9.29, 25.1, 39.8, 55.9, 60.4, 63.9, 69.2 and 72.4.

*3-hydrazinyl-4-hydroxymethyl-1-methyl-5-(4-ethoxy phneyl)pyrrolidine (**CoS-10**)*. Brown solid; 80%. HRESI-MS (negative mode) *m/z*: $[M]^-$ 251.1182 (Calc. for $C_{13}H_{21}N_3O_2$, 251.1639). ^{1}H-NMR (CD_3OD, 400 MHz) δ 2.06 (3H, s, NCH_3), 2.50 (1H, *dd*, *J*= 6.0, 11.2 Hz, CH), 2.91 (1H, *d*, *J*= 9.6 Hz, NCH_2-a), 3.01 (1H, *d*, *J*= 10.8 Hz, NCH_2-b), 3.39 (1H, *dd*, *J*= 6.0, 11.6 Hz, OCH_2-a), 3.60 (1H, *dd*, *J*= 4.4, 11.6 Hz, OCH_2-b), 3.75 (3H, *s*, OCH_3), 4.21 (1H, *m*, NHCH), 6.87 (2H, *d*, *J*= 8.8 Hz, Ar-CH) and 7.31 (2H, *d*, *J*= 8.8 Hz, Ar-CH). ^{13}C-NMR (CD_3OD, 100 MHz) δ 39.2, 54.4, 59.7, 60.0, 64.5, 71.5, 72.9, 113.6, 129.2, 131.8 and 159.5.

*3-hydroxy-5-(4-methoxyphneyl) pyrrolidine (**CoS-11**)* Pale brown solid; 85%. HRESI-MS (negative mode) *m/z*: $[M]^-$ 207.0912 (Calc. for $C_{12}H_{17}NO_2$, 207.1265). ^{1}H-NMR (CD_3OD, 400 MHz) δ 2.04 (3H, *s*, NCH_3), 2.38 (1H, *m*, CH_2-a), 2.52 (1H, *dt*, *J*= 7.6, 14.0 Hz,

CH_2-b), 3.50 (1H, *dd*, *J*= 7.2, 9.6 Hz, NCH_2-a), 3.50 (1H, *dd*, *J*= 6.8, 10.4 Hz, NCH_2-b), 3.74 (3H, *s*, OCH_3), 4.29 (1H, *m*, NCH), 4.39 (1H, *m*, CHOH), 6.84 (2H, *d*, *J*= 8.8 Hz, Ar-CH) and 7.27 (2H, *d*, *J*= 8.8 Hz, Ar-CH). ^{13}C-NMR (CD_3OD, 100 MHz) δ 39.2, 44.8, 54.4, 65.4, 68.6, 70.9, 113.5, 128.7, 131.2 and 159.5.

RESULTS AND DISCUSSION

The investigation of antidiabetic potential of pyrrolidine-based iminosugars in this study began with the design and synthesis of new analogues based on modifications of the core structures of iminohexitol and iminoarabinitol (**Fig. 1**). The modifications were set out to explore the impact of chemical diversity on the pyrrolidine rings to their molecular docking and bioactivity properties.

1. Chemical Synthesis

The general synthesis route towards our targeted iminosugar derivatives involved one-pot amination and cyclization, hydroxylamination, hydrazinylation, and reduction, as shown in **Scheme 1**. Synthesis of analogues **CoS (1-11)** proceeded trough the key ethyl 3-hydroxy-4-pyrrolidinecarboxylate intermediates **1**, which were obtained via one-pot amination and cyclization of three components; diethyl oxaloacetate, formaldehyde, and ammonia as reported by Muhammad *et al*., 2009. In this synthesis, reaction of sodium diethyl oxaloacetate with amines (ammonia and methylamine), and aldehydes (formaldehyde, acetaldehyde, ethanaldehyde, and *p*-methoxyben-zaldehide) gave the respective intermediates **1a-e** in moderate yields. Treatment of intermediate **1a** with hydroxylamine hydrochloride in the presence of a base gave ethyl 3-hydroxyamino-4-pyrrolidinecarboxylate **2a**, and treatment of intermediates **1a-e** with hydrazine in ethanol under reflux condition gave appropriate ethyl 3-hydrazinyl-4-pyrrolidinecarboxylates **3a-e** in moderate to good yields. Besides that, decarboxylation of intermediate **1e** using 10% aqueous HCl under reflux condition directly led to pyrrolidinone intermediate **4a**.

Compounds **1-4** served as important intermediates in the preparation of our target compounds, as direct reduction of **1-4** led to our target iminosugar derivatives (**Fig. 2**). However, due to the regulated *cis*-orientation of protons at C-3 and C-4 positions, reduction of C3-C4 double bond using H_2 Pd/C was needed prior to reduction of ester and amide groups with $LiAlH_4$. In this strategy, series of reductions of intermediates **1-4** using H_2 Pd/C in the presence of catalytic amount of acetic acid, followed by reductions using excess $LiAlH_4$ gave respective iminosugar analogues **CoS** (**1-11**) in good yields. Chemical structures of all targeting compounds and their intermediates have been proven by their spectral data evidence.

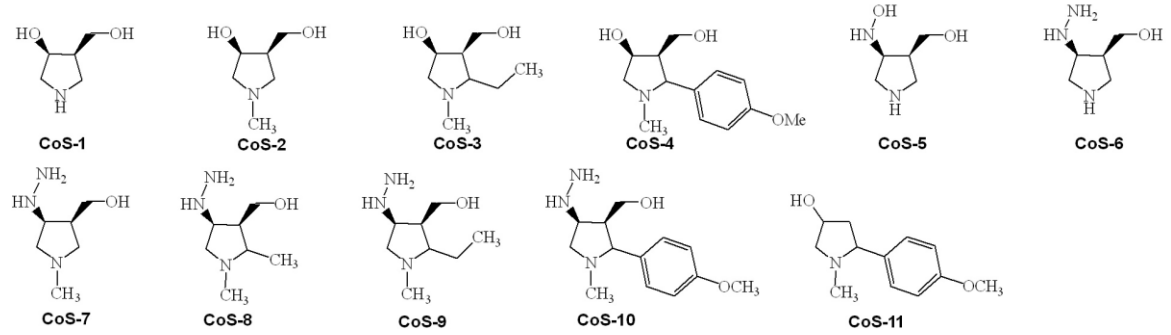

Figure 2. Chemical structures of target pyrrolidine-based iminosugar derivatives

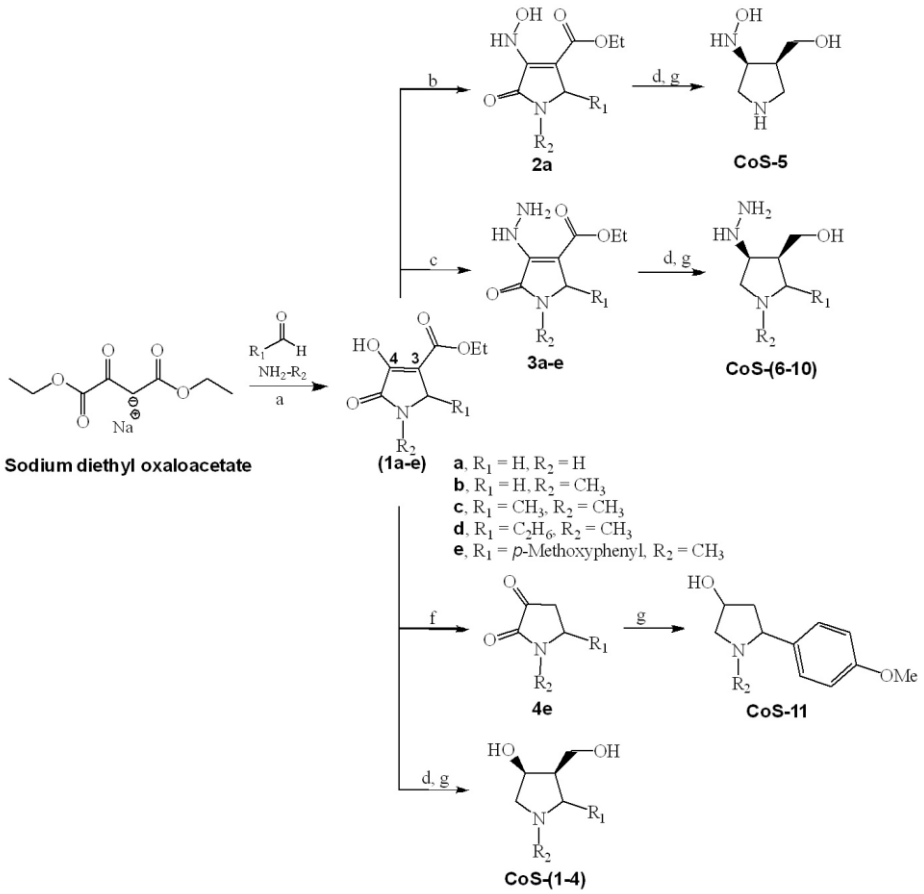

Scheme 1. Reagents and conditions: (a) EtOH, reflux 0.5-1 h; (b) $NH_2OH.HCl$, $NaHCO_3$, Na_2SO_4, DCM, rt, 24 h; (c) NH_2NH_2, EtOH, rt, 30 min; (d) H_2 Pd/C, EtOH, rt, 24 h; (f) 10% HCl, reflux 7 h; (g) $LiAlH_4$, ether, 60 ^oC, 11 h.

Table 1. α-Glucosidase inhibition studies of pyrrolidine-based iminosugars (**CoS 1–CoS 11**).

Compound	IC_{50} (mM)[1]	Glide score (kcal/mol)
DNJ	0.558 ± 1.030	-5.735
CoS 1	1.404 ± 1.005	-5.382
CoS 2	2.938 ± 1.076	-3.523
CoS 3	1.800 ± 1.016	-3.459
CoS 4	1.660 ± 1.017	-3.436
CoS 5	2.171 ± 1.365	-4.860
CoS 6	1.751 ± 1.006	-3.778
CoS 7	1.311 ± 1.003	-4.248
CoS 8	1.271 ± 1.859	-3.705
CoS 9	1.523 ± 1.006	-3.589
CoS 10	1.116 ± 1.010	-4.436
CoS 11	1.169 ± 1.012	-3.699

[1]Data are expressed as mean ± S.D., n = 3.

2. α-Glucosidase Inhibitory Activity

All the newly synthesized compounds (**CoS 1 - CoS 11**) were evaluated for their inhibitory potential against α-glucosidase as shown in **Table 1**. 1-Deoxynojirymycin (**DNJ**), an established α-glucosidase inhibitor, was used as the positive control. Among the tested analogues, **CoS 1-11** showed variable degrees of α-glucosidase inhibition with IC_{50} values ranging between 1.116 ± 1.010 mM and 2.938 ± 1.076 mM as compared with DNJ (IC_{50} = 0.558 ± 1.030 mM). **CoS 10** was found to be the most potent compound in the series. This compound has hydrazine group at C-4 and methoxybenzene group at C-2 which seemed to play important roles in the inhibition activity. However, replacing hydrazine group with hydroxyl group and removing hydroxymethyl group led to a slight decline in the activity of **CoS 11**, the second most active compound. This might be due to the lack of electron donating ability. Replacing a methoxybenzene with methyl in **CoS 8** showed a reduction in the inhibitory activity.

This was because there was less hydrophobic interaction in the active site. However, the extra methyl group slightly enhanced the activity of **CoS 8** as compared to **CoS 7**. Longer alkyl group at C-2 otherwise reduced the potency of **CoS 9**. Among the iminosugars, **CoS 1** with no substitution had the highest inhibitory activity because the compound highly mimicked the structure of the substrate, thus it fitted well in the active site. The substitution of methyl group at amine-membered ring and hydroxyamino group at C-3 position caused a huge decrease in activity in **CoS 2** and **CoS 5**, respectively. In contrast, addition of *p*-methoxybenzene ring at C-2 increased the activity of **CoS 4**. However, **CoS 3** which has ethyl substitution at C-2 exhibited lower activity as compared to **CoS 4**. Overall, the order of synthesized pyrrolidine-based iminosugars based on IC_{50} values is as follows: **CoS 2** < **CoS 5** < **CoS 3** < **CoS 6** < **CoS 4** < **CoS 9** < **CoS 1** < **CoS 7** < **CoS 8** < **CoS 11** < **CoS 10**. To understand the mechanism of enzyme inhibition and binding interaction of these analogues in the binding pockets of α-glucosidase, molecular docking studies were performed.

3. Homology Modelling

To investigate the inhibitory activity of the synthesized compounds against α-glucosidase, a homology modelling of α-glucosidase from *Saccharomyces cerevisiae* was used since the crystal structure of the enzyme has never been resolved experimentally yet. Crystallographic structure of *Saccharomyces cerevisiae* isomaltase (PDB ID:3AJ7) was chosen as the template for homology model based the highest of sequence similarity (71.92%) and lowest resolution (1.3 Å). The alignment sequence showed that the catalytic domain was conserved in both proteins.

The quality of the modelled structure was validated by Ramachandran plot using RAMPAGE (http://mordred.bioc. cam.ac.uk/~rapper/rampage. php). Based on Ramachandran plot, 97.8% of residues were located in the most favored zone, 2.1% of residues in allowed regions and only 0.2% of residues in disallowed regions. The good results obtained from the Psi/Phi Ramachandran plot suggested that the homology model of α-glucosidase can be used for docking studies. The folding of protein structure of homology model and X-ray crystal structure were also quite similar as inferred in superimposed structure. However, there was narrower opening to active site in modelled α-glucosidase than isomaltase due to the presence of His239 and Glu304.

4. Docking Study

Molecular docking study was conducted to investigate the binding mode of the synthesized compounds within the binding site. From the docking results, no definite agreement was observed between Glide score and IC_{50} of the pyrrolidine-based iminosugars but active compounds showed stable binding mode within active site of α-glucosidase in comparable with the standard drug, **DNJ** (**Table 2**). The binding modes were able to discriminate between the most and least active compounds. The most active compounds (**CoS 4, 10**) were bound at the middle depth of the binding pocket which was near the opening of the active site (**Fig. 3**). Interestingly, the least active compounds (**CoS 1, 2, 3, 5, 6, 7, 8, 9, 11**) were bound at the bottom of the active site pocket where the catalytic site of the enzyme was located. Furthermore, these compounds orientated in a similar fashion with **DNJ** at the same site. Therefore, the compounds were postulated to act as competitive inhibitors to the substrate of α-glucosidase, maltose.

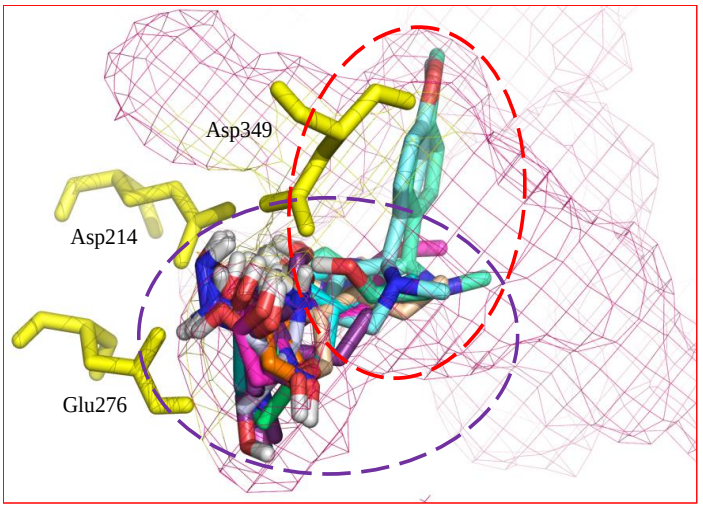

Figure 3. The comparison of binding pose of compounds **CoS 1-11** in the binding site of α-glucosidase (Red circle line= most active; Purple circle line= least active; Yellow stick= catalytic residues.

The theoretical binding pose of **DNJ** is presented in **Fig. 4a**. **DNJ** was well accommodated at the deep site of binding pocket. It established eight H-bond interactions and was stabilized by four hydrophobic residues, which were Tyr71, Phe158, Phe177, and Phe300. It was shown that catalytic residue Asp349 made H-bond with hydroxyl group whereas residues Asp214 and Glu276 made H-bonds with *N*-membered benzene ring. Glu276 also interacted with hydroxyl group to form H-bond. Other H-bond interactions were formed between hydroxyl group of benzene ring and Asp68, His111, and Arg439. The interactions observed were reported in the literature [18]. The most active compound, **CoS 10** was oriented in a different position as the standard drug (**Fig. 4k**). The methoxybenzene ring was projected towards the small side pocket near the entrance of the active site whereas the pyrrolidine ring was positioned at the middle of the active site pocket. The orientation gave an advantage to the compound in building a strong π-π interaction between the phenyl ring and Phe300. In addition, -OH and -NH_2 of the compound made H-bond interactions with an important residue, Glu276 and *O*-methoxyl group formed a H-bond interaction with Gln350. Phe157, Phe158, Phe177, Phe300, and Val303 stabilized the compound inside the binding pocket. The second most active compound, **CoS 11** possessed different binding modes as in **CoS 10** (**Fig. 4l**). The lack of substitution groups at C-3 and C-4 of the pyrrolidine ring caused it to bind deeply into the active site. Its pyrrolidine ring fitted in a similar manner as DNJ while the methoxybenzene ring was projected towards the opening of the active site. Two H-bonds were formed between the hydroxyl group attached to the pyrrolidine ring and *N*-methyl of pyrrolidine ring. Its binding interactions were stabilized by Tyr71, Phe157, Phe158, Phe177, and Phe300. The presence of five benzyl ring gave strong hydrophobic interactions in the stabilized protein-ligand complex. **CoS 7-9** also exhibited good biological activities against the enzyme but showed less inhibitory activities compared to **CoS 10** and **CoS 11** due to the presence of benzyl ring at the same position. In this case, **CoS 7-9** formed five, four, and three H-bond interactions, respectively. Asp214 formed two H-bond interactions with two nitrogens of hydrazine group and Glu276 established two H-bond interactions with hydroxyl group and -NH_2 group in **CoS 7**. Another H-bond interaction was formed between Asp349 and -NH_2 group in **CoS 7.** Similarly, Glu276 and Asp349 formed H-bond interactions with each nitrogen in hydrazine group in **CoS 8** and Asp68 and Arg439 made H-bond interactions with the same hydroxyl group. In contrast, out of four H-bond interactions in **CoS 8** only Arg439 did not form any interaction in **CoS 9** which resulted in the reduction of its activity. The interactions of these compounds are illustrated in **Fig. 4h-j**.

The binding mode of pyrrolidine-based iminosugar, **CoS 1** is theoretically presented in **Fig. 4b**. **CoS 1** had a favorable binding mode as in **DNJ**. Five H-bond interactions were found in **CoS 1** which involved Asp68, Asp214, Asp349, His348, and Arg439. The orientation of **CoS 2** was changed with the extra methyl group at *N*-membered ring which caused less formation of H-bond and influenced its activity. It was found that three H-bonds were formed with each of Asp214 (*N*-membered ring), Glu276 (hydroxymethyl), and Asp349 (hydroxyl) (**Fig. 4c**).

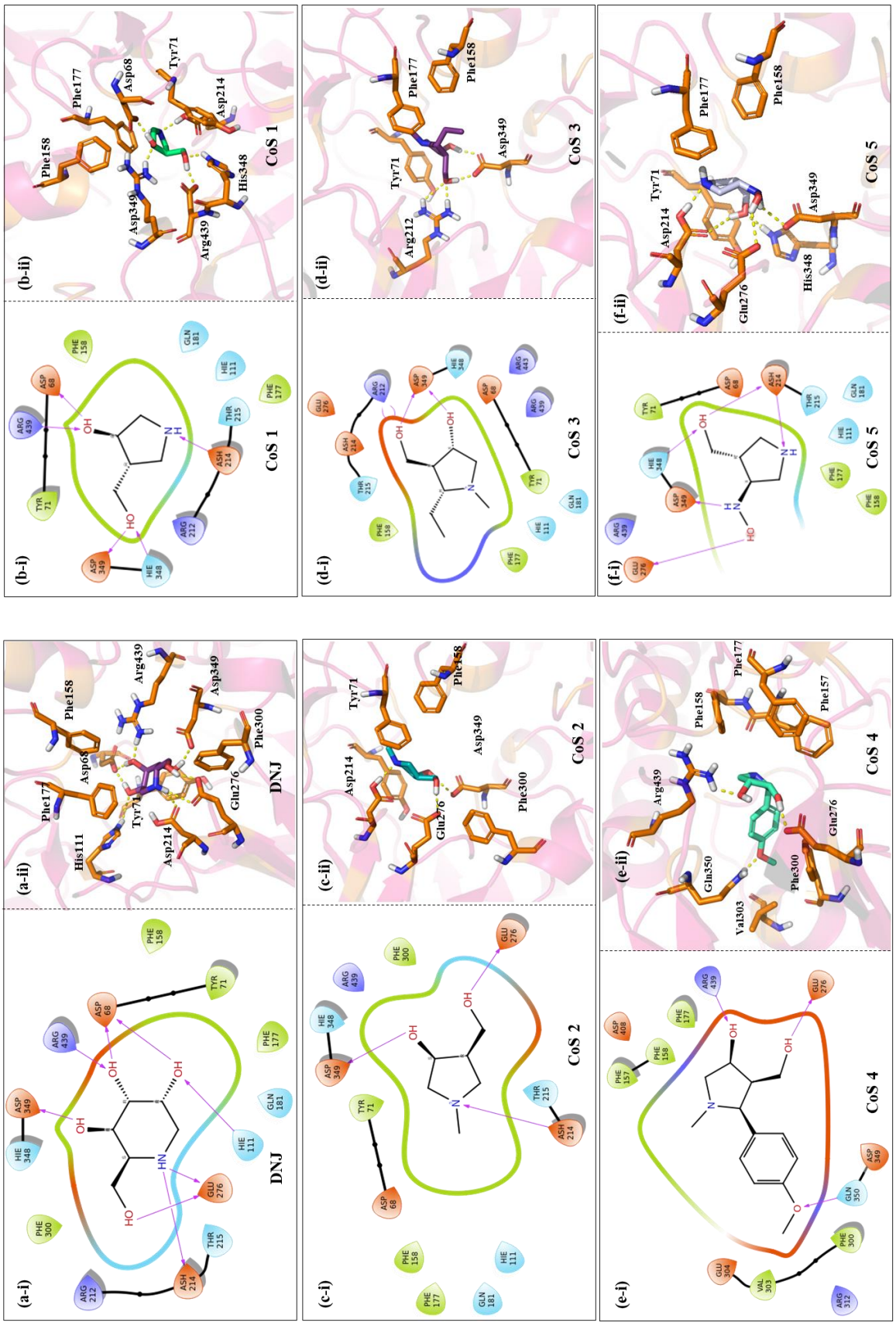

Figure 4. The binding interaction of compounds as generation using Ligand Interaction Diagram (i) and binding pose as analyzed using Pymol (ii). (a) **DNJ**, (b) **CoS 1**, (c) **CoS 2**, (d) **CoS 4**, (e) **CoS 5**, (f) **CoS 6**, (g) **CoS 7**, (h) **CoS 8**, (i) **CoS 9**, (j) **CoS 10**, (k) **CoS 11**, and (l) **CoS 12**. Arrows (magenta) and dashed lines (yellow) denote H-bond interactions and green lines represent π-π interactions. Green petals are hydrophobic residues, light blue petals are polar residues, brown petals are negative charged amino acids, and blue petals are positive charged amino acids.

Figure 4 (continues)

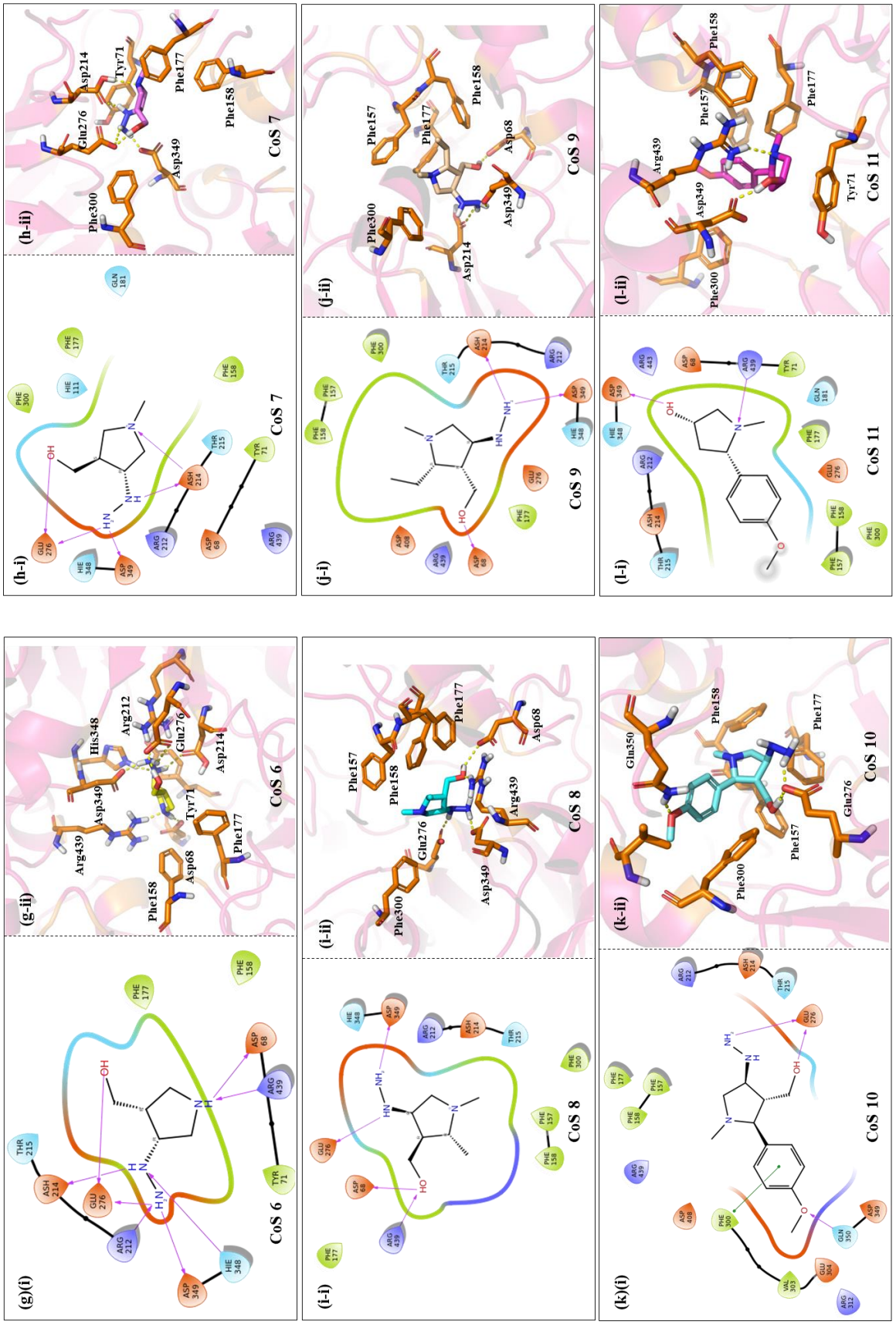

Both compounds were stabilized by the same residues (Tyr71, Phe158, Phe177) and Phe300 in **CoS 2** only. The addition of hydroxyamino group in **CoS 5** also caused changes in the compound orientation. Although the number of its H-bond interaction was the same as that of **CoS 1**, less hydrophobic interactions were formed (**Fig. 4f**). Five H-bond interactions in **CoS 1** originated from the interaction of hydroxymethyl group and Asp214 and His348, *N*-membered ring and Asp214, OH-amino group and Glu276, and *NH*-amino group and Asp349. Residues that were involved in hydrophobic interactions were Tyr71, Phe158, and Phe177. It is noteworthy that the introduction of a more electronegative group (hydrazinyl group) had a great impact in improving the activity of **CoS 6** as it increased the number of H-bond interactions (**Fig. 4g**) to eight H-bonds. Residues of the active site (Arg212, Asp214, Glu276 and Asp349) were mainly interacted with the hydrazinyl group. Other H-bond interactions were those between hydroxymethyl group and Glu276 and between NH-membered ring and Asp68 and Arg439. On the other hand, the substitution at C-2 position of **CoS 3** and **CoS 4** also improved the activity as compared to **CoS 2**. This fact strengthened the importance of substituent at this position. Four and three H-bond interactions were found in **CoS 3** and **CoS 4**, respectively, but **CoS 4** was more stable than **CoS 3** because of the presence of more hydrophobic interactions surrounding the compound. In **Cos 3**, the hydroxymethyl group interacted with Arg212 and Asp349 to form H-bonds and the hydroxyl group interacted with the same Asp349 to form another H-bond (**Fig. 4d**). In contrast, **CoS 4** oriented as observed in **CoS 10**. As a result, Arg439, Glu276, and Gln350 established H-bond interactions with the hydroxyl, hydroxymethyl, and *O*-methoxyl group, respectively, in **CoS 4** (**Fig. 4e**). In summary, the attachment of a strong electron donating group (hydrazine) C-4 position of pyrrolidine ring and phenyl ring played important roles in determining the potency and characteristics of the compounds. Hence, these moieties need to be considered in designing α-glucosidase inhibitors. Moreover, the inhibitors should occupy both parts of the active site.

5. Pharmacokinetic Properties

The calculated physicochemical properties indicated that all the synthesized compounds had drug-like properties (**Table 2**) and the descriptors fell within 95% range values of known drugs (**Table 3**). Moreover, most of the compounds were orally bioavailable and would be easily absorbed as they were likely to be membrane permeable. Only **CoS 7**, **CoS 8**, **CoS 9**, **CoS 10**, and **Cos 11** possessed low values for QPPCaco between 4.385 nm/sec to 12.324 nm/sec and low percentage of human oral absorption (less than 50%). Despite being biologically active, **CoS 11** has higher chance to cause cardiac hERG (human *Ether-à-go-go*-Related Gene) potassium channel blockage compared to the other compounds.

Table 2. Drug-likeness of the synthesized compounds (Lipinski's Rule of Five)

Comp.	MW	Donor HB	Accept HB	QP log Po/w
CoS 1	117.147	3	4.90	-1.139
CoS 2	132.162	2	5.40	-0.723
CoS 3	131.174	2	5.40	-0.141
CoS 4	237.298	2	6.15	0.851
CoS 5	145.201	4	5.90	-1.530
CoS 6	159.228	5	4.70	-2.483
CoS 7	251.328	4	5.20	-1.910
CoS 8	159.231	4	5.20	-1.676
CoS 9	173.258	4	5.20	-1.380
CoS 10	251.328	4	5.95	-0.427
CoS 11	207.272	1	4.45	1.456

Molecular weight (MW): value must be below 500. Average number of hydrogen bond donor taken over a number of configurations (donor HB): value must be 5 or below. Average number of hydrogen bond donor taken over a number of configurations (donor HB): value must be 10 or below. Predicted octanol/water partition coefficient (QP log Po/w): value must be below 5.

Table 3. Pharmacokinetic predictions of compounds

Comp.	#stars	Rule of Five	QP log S	#metab	QPPCaco (nm/sec)	QP log BB	QPPMDCK (nm/sec)	Percent Human Oral Absorption	Q Plog HERG
CoS 1	5	0	0.682	2	160.073	-0.158	75.542	59.729	-3.178
CoS 2	2	0	0.440	3	277.226	0.007	136.773	66.432	-3.412
CoS 3	1	0	0.089	3	347.117	0.026	174.397	71.587	-3.415
CoS 4	0	0	-1.188	5	377.889	-0.010	191.166	78.056	-4.653
CoS 5	4	0	0.597	1	84.467	-0.443	37.853	52.468	-3.213
CoS 6	4	0	2.000	1	4.385	-0.127	1.894	23.897	-4.788
CoS 7	2	0	2.000	2	9.803	0.130	4.518	33.506	-4.980
CoS 8	2	0	2.000	2	9.574	0.125	4.403	34.691	-4.953
CoS 9	2	0	2.000	2	11.704	0.155	5.471	37.985	-4.801
CoS 10	1	0	0.756	4	9.767	-0.051	4.499	42.16	-6.360
CoS 11	0	0	-1.083	4	813.124	0.409	437.643	87.557	-4.710

Number of property or descriptor values that fall outside the 95% range of similar values for known drugs (#stars): range of recommended value is between 0 to 5. Number of violations of Lipinski's rule of five (Rule of Five): no violation of rule of five is accepted. Predicted aqueous solubility (QP log S): value less than -6 or greater than -1 is undesirable. Number of likely metabolic reactions (#metab): recommended value between 1 to 8. Predicted apparent Caco-2 cell permeability (QPPCaco): value less than 25 is undesirable. Predicted brain/blood partition coefficient (QP log BB): recommended value is between -3.0 to 1.2. Predicted apparent MDCK cell permeability (QPPMDCK): <25 poor, >500 great. Predicted human oral absorption (Percent Human Oral Absorption): value less than 25% indicates poor absorption. Predicted IC_{50} value for blockage of HERG K^+ channels (QP log HERG): value below -5 is undesirable.

CONCLUSION

Diverse scaffolds of pyrrolidine-based iminosugars were successfully synthesized with good yields. The α-glucosidase inhibitory activity of these derivatives was evaluated. The key structural elements in binding interaction were identified through structure activity relationship and further rationalized using *in silico* studies. Overall, this study demonstrated that the newly synthesized compounds had promising effects in inhibiting α-glucosidase and further optimization can be done to improve their activity.

ACKNOWLEDGEMENT

The author would like to thank the generous support of Institute of Science (IOS), UiTM Shah Alam, Malaysia, Prof. Dr Mohd Zaki Bin Salleh, Muhd Hanis Md Idris and Muhd Izwan Muhd Yusof from Integrative Pharmacogenomics Institute (iPROMISE), UiTM Selangor, Malaysia for technical assistance in molecular modelling and mass spectrometer measurement of samples. The Ministry of Higher Education (MOHE), Malaysia for the financial support under the Fundamental Research Grant Scheme (Grants No.: 600-RMI/FRGS 5/3 (109/2019) and 600-RMI/ST/FRGS 5/3/(0071/2016)) and Transdisciplinary Research Grant Scheme (Grant No.: 600-RMI/TRGS 5/3 (1/2014)).

REFERENCES

1. Doddi, V. R. and Y. D. Vankar (2007) Synthesis of Pyrrolidine-Based Imino Sugars as Glycosidase Inhibitors. *European Journal of Organic Chemistry*. **2007**, 5583–5589.

2. Lillelund, V. H., et al. (2002) Recent Developments of Transition-State Analogue Glycosidase Inhibitors of Non-Natural Product Origin. *Chemical Reviews*. **102**, 515–554.

3. Karaveg, K., et al. (2005) Mechanism of Class 1 (Glycosylhydrolase Family 47) α-Mannosidases Involved in N-Glycan Processing and Endoplasmic Reticulum Quality Control. *Journal of Biological Chemistry*. **280**, 16197–16207.

4. Doddi, V. R. and Y. D. Vankar (2007) Synthesis of Pyrrolidine-Based Imino Sugars as Glycosidase Inhibitors. *European Journal of Organic Chemistry*. **2007**, 5583–5589.

5. Donohoe, T. J., et al. (2004) Enantioselective Partial Reduction of 2,5-Disubstituted Pyrroles via a Chiral Protonation Approach. *Organic Letters*. **6**, 3055–3058.

6. Cren, S., C. Wilson, and N. R. Thomas (2005) A Rapid Synthesis of Hexofuranose-like Iminosugars Using Ring-Closing Metathesis. *Organic Letters*. **7**, 3521–3523.

7. Carmona, A. T., et al. (2003) Stereoselective Syntheses of 1,4-Dideoxy-1,4-imino-octitols and Novel Tetrahydroxyindolizidines. *The Journal of Organic Chemistry*. **68**, 3874–3883.

8. Lindstrom, U. M., R. Ding, and O. Hidestal (2005) Efficient asymmetric synthesis of an azasugar in water. *Chemical Communications*, 1773–1774.

9. Ayad, T., et al. (2003) A Flexible Route Towards Five-Membered Ring Imino Sugars and Their Novel 2-Deoxy-2-fluoro Analogues. *European Journal of Organic Chemistry*. **2003**, 2903–2910.

10. Shaameri, Z., et al. (2016) Synthesis of 3,4-Fused γ-Lactone-γ-Lactam Bicyclic Moieties as Multifunctional Synthons for Bioactive Molecules. *Journal of Heterocyclic Chemistry*. **53**, 1059–1064.

11. Mohammat, M. F., et al. (2015) Diastereo-selective Reduction of 2,3-Dioxo-4-carboxy-5-substituted Pyrrolidines Using NaBH4/AcOH and Heterogenous Hydrogenation Reactions. *Journal of the Korean Chemical Society*. **59**, 31–35.

12. Shaameri, Z., et al. (2013) A Short and Elegant Synthesis of (±)-Streptopyrrolidine. *Journal of Heterocyclic Chemistry*. **50**, 320–325.

13. Mohammat, M., Z. Shaameri and A. Hamzah (2009) Synthesis of 2,3-Dioxo-5-(substituted)arylpyrroles and Their 2-Oxo-5-aryl-3-hydrazone Pyrrolidine Derivatives. *Molecules*. **14**, 250.

14. Mohalid, N., A. S. Hamzah, and Z. Shaameri (2015) Chemical exploration of 4-hydroxybenzylated 3-substituted tetramic acid. *Malaysian Journal of Analytical Sciences*. **19**, 359–368.

15. Wibowo, A., et al. (2017) Asymmetric Reduction of 3-Ketoproline Ethyl Ester by Modified Borohydrides and Various Vegetables. *Journal of the Korean Chemical Society*. **61**, 244–250.

16. Sievers, F., et al. (2011) Fast, scalable generation of high-quality protein multiple sequence alignments using Clustal Omega. *Molecular Systems Biology*. **7**, 539.

17. Lee, S. S., H. C. Lin and C. K. Chen (2008) Acylated flavonol monorhamnosides, α-glucosidase inhibitors, from Machilus philippinensis. *Phytochemistry*. **69**, 2347–2353.

18. Keizo, Y., et al. (2010) Crystal structures of isomaltase from Saccharomyces cerevisiae and in complex with its competitive inhibitor maltose. *The FEBS Journal*. **277**, 4205–4214.